PREDICTION OF VORTEX BREAKDOWN ON A DELTA WING

S. Agrawal*
B. A. Robinson**
R. M. Barnett†

McDonnell Aircraft Company
McDonnell Douglas Corporation
St. Louis, Missouri 63166

Abstract

Recent studies of leading-edge vortex flows with computational fluid dynamics codes using Euler or Navier-Stokes formulations have shown fair agreement with experimental data. These studies have concentrated on simulating the flowfields associated with a sharp-edged flat plate 70° delta wing at angles of attack where vortex breakdown or burst is observed over the wing. There are, however, a number of discrepancies between the experimental data and the computed flowfields. The location of vortex breakdown in the computational solutions is seen to differ from the experimental data and to vary with changes in the computational grid and freestream Mach number. There also remain issues as to the validity of steady-state computations for cases which contain regions of unsteady flow, such as in the post-breakdown regions. As a partial response to these questions, a number of laminar Navier-Stokes solutions have been examined for the 70° delta wing. The computed solutions are compared with an experimental database obtained at low subsonic speeds. The convergence of forces, moments and vortex breakdown locations are also analyzed to determine if the computed flowfields actually reach steady-state conditions.

Introduction

High angle of attack maneuvering has become an integral part of the flight envelopes for current and future fighter aircraft. At such flight conditions vortical flow is a dominant feature of the flowfield. Vortex flows include complex features such as massive flow separation, and breakdown or bursting of vortices, that are not well understood at present and are topics of active research. The bursting of the vortex may result in several adverse effects, such as an abrupt change in pitching moment, loss in lift, and buffet, and can be a strict limitation of its maneuverability. Predicting and understanding such flowfields is, therefore, very important.

Vortex breakdown or burst is characterized by a sudden deceleration of the axial flow in the vortex core, and a decrease in the circumferential velocity associated with the rapid expansion of the vortex core (Ref 1). The vortex burst phenomenon has been the subject of much study, both experimentally (Refs 1,2) and theoretically (Refs 3,4) for more than two decades. A detailed survey of the research conducted in this subject area is provided in Refs 2-4. The theoretical studies thus far have been for relatively simple cases, such as a vortex confined in a tube, or an isolated vortex. Although many experiments have been performed to help understand breakdown, there is still no general agreement regarding the essential mechanism of vortex breakdown, and no reliable criterion is available to predict vortex breakdown location for a broad range of geometries and flight conditions.

A flat plate delta wing with sharp leading edges presents a simple configuration for the study of vortical flows, including breakdown. Several investigators have analyzed the flowfields past delta wings at high angles of attack, both experimentally (Refs 5-7) and numerically (Refs 8-13). Numerical investigations have been carried out using both Euler and Navier-Stokes formulations. It has been shown that vortex trajectories are predicted quite well, at least in the pre-breakdown regions, using both Euler and Navier-Stokes equations for a sharp-edged delta wing (Ref 12). Breakdown locations are predicted somewhat better using the Navier-Stokes equations, although correlation between the computed and experimental data for breakdown locations is still inadequate.

The majority of studies reported in the literature are based on steady-state calculations, primarily due to the enormous computation time associated with time-accurate solutions. Since the flowfield in the post-breakdown region is inherently unsteady, caution must be exercised in interpreting steady-state results. Flowfields predicted in the vortical flow region are found to be strongly dependent on the grid density. For adequate resolution of the vortical flowfields, a large number of grid points are required, thus increasing the computational time proportionately. Compressibility also plays a role in modifying the structure of the leading-edge vortex, and thereby its breakdown location. These are the issues that are addressed in this paper using computational solutions. Specifically, the effects of compressibility and grid enrichment on vortex breakdown locations are discussed. Although only steady-state solutions of the Navier-Stokes equations are used to characterize flowfields, issues related to unsteady effects are also addressed.

Grid Topology and Numerical Method

An H-O type grid topology for a half-plane model of the delta wing was used in this study. Figure 1 shows the geometry used in this study. Only cases without sideslip were considered, so a half-plane wing provided the best grid resolution

---

* Technical Specialist - Aerodynamics
** Engineer - Aerodynamics
† Senior Engineer - Aerodynamics

around the wing for a given number of points. For most calculations, the grid dimensions were 61 (axial), 65 (radial), and 89 (circumferential), with 41 points along the wing in the chordwise direction. This grid will be referred to as the medium grid in this paper. A grid embedding technique was also utilized to refine the medium grid around the leading edge and the upper surface of the wing from the apex to the trailing edge. The extent of embedding in the normal direction was just far enough to include the region where most of the vortical flow phenomena was observed. This refinement of the medium grid yielded an embedded region with dimensions of 81 (axial), 87 (radial), and 133 (circumferential).

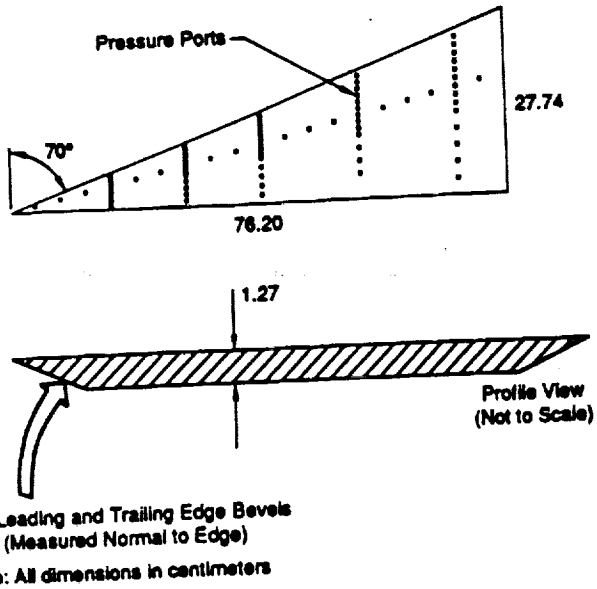

Fig. 1 Flat Plate Semispan Delta Wing Model

The grid was constructed by successive generation of two-dimensional (2-D) grids normal to the wing centerline. These 2-D grids were generated using a method that solves an elliptic system of partial differential equations (Ref 14). This procedure results in a high quality, orthogonal grid, even near difficult areas such as the sharp leading edge of the wing.

The CFL3D Euler/Navier-Stokes code (Ref 15) was used to calculate all of the flowfields in this study. The computational algorithm is based on a thin-layer approximation to the three-dimensional, time-dependent, conservation law form of the compressible Navier-Stokes equations. The code solves the discretized flow equations implicitly using an upwind-biased spatial differencing scheme with either flux difference splitting or flux vector splitting for the convective and pressure terms, and central differencing for the shear stress and heat transfer terms. In this study, the Roe-averaged flux difference splitting is applied for the spatial terms. Flux limiting is also used to alleviate oscillations near high gradient flow regions.

Rossby Number

As the Rossby number has been used in analyzing the majority of results in this paper, a brief discussion of this number is in order here. It is a parameter which is essentially a ratio of the axial and the circumferential momentum in a vortex. A standard definition (Ref 16) is:

$$Ro = \frac{U}{r\,\Omega}$$

where U is the core axial velocity, Ω is the rotation rate, and r is an effective radius of the vortex. For a mathematical model these three quantities may be determined analytically, whereas for experimental and numerical solutions an integral-based approach is used. In this approach, a non-dimensional vorticity (ω) is calculated for each cell using Stokes theorem. An area (A) of the primary vortical region is defined by the cells that have $\omega \geq 1$. This value of ω was chosen empirically. The rotation rate and effective radius are then calculated as

$$\Omega = \frac{\Sigma\ \omega\ dA}{2A}, \quad r = \sqrt{\frac{A}{\pi}}$$

The axial velocity is calculated by integrating the velocity component, v', along the vortex axis, over an area defining the vortex core, A'.

$$U = \frac{\Sigma\ v'\ dA'}{\Sigma\ dA'}$$

The area A' is defined by a circle centered at the centroid of vorticity ($\omega \geq 1$) with some small radius consistent with the size of the vortex. This procedure results in a numerically-determined Rossby number. Through correlations with other methods of determining breakdown and experimental data on the flat plate delta wing, it has been found that Rossby numbers corresponding to burst locations are near 1.0 (Ref 13). In the pre-breakdown regions, Ro is usually high (above 1.8). In the post-breakdown regions, it is usually small (below 0.9) in which case the vortex will not be stable.

Results

The numerical results presented here have been obtained using the CFL3D code. Calculations were performed at several angles of attack. Due to similarity of the solutions, results are shown only for an angle of attack of 30°. An earlier investigation focused on the vortex breakdown prediction using Euler and Navier-Stokes (laminar and turbulent) solutions on the delta wing. We observed that the laminar results overall provided the best comparison with the test data (Ref 12). Therefore, only laminar solutions were attempted in this study. The Reynolds number based on the root chord (Re) was held constant at one million. Calculations at Mach numbers from 0.1 to 0.4 were performed to address the effects of compressibility on the vortical flow and breakdown position. The pre- and post-breakdown flowfield regions were examined using the Rossby number analysis (Ref 13) to investigate flowfield unsteadiness. Also, grid embedding was used to examine grid enrichment effects on predicted vortex breakdown location. Comparisons between the computed and the wind tunnel test data are shown wherever applicable. The test database consists of surface pressures,

three-component Laser Doppler Velocimetry (LDV) and seven-hole probe flowfield surveys (Ref 17).

Mach Number Effects

The experimental data used for comparison in this study were obtained at a very low freestream Mach number ($M_\infty \leq 0.05$). It is difficult or sometimes impossible to solve these low speed flows with a compressible CFD code since the solution may converge only after a prohibitively large number of iterations. Therefore, earlier numerical investigations (Ref 12) on this geometry were conducted at a freestream Mach number of 0.3, for efficiency considerations.

Even at a relatively low freestream Mach number, the local Mach number in the vortex core may extend into the compressible range. This is due to the accelerated flow at the core of the vortex which may experience local Mach numbers two to three times the freestream value (Ref 17). To determine if compressibility indeed affects the vortex breakdown location, computed solutions at four different freestream Mach numbers (M_∞ = 0.1, 0.2, 0.3, and 0.4) were analyzed on the medium grid. Figure 2 shows the effect of freestream Mach number on the local Mach number in the vortex at 25% root chord. It is apparent that the flow in the core of the vortex shown in Figures 2c-2d, corresponding to M_∞ = 0.3 and 0.4, is well into the compressible range (local Mach number ≥ 0.7). In fact, for M_∞ = 0.4 it reaches the sonic condition. It is interesting to note that for all cases the local maximum Mach number is about two and a half times the freestream value.

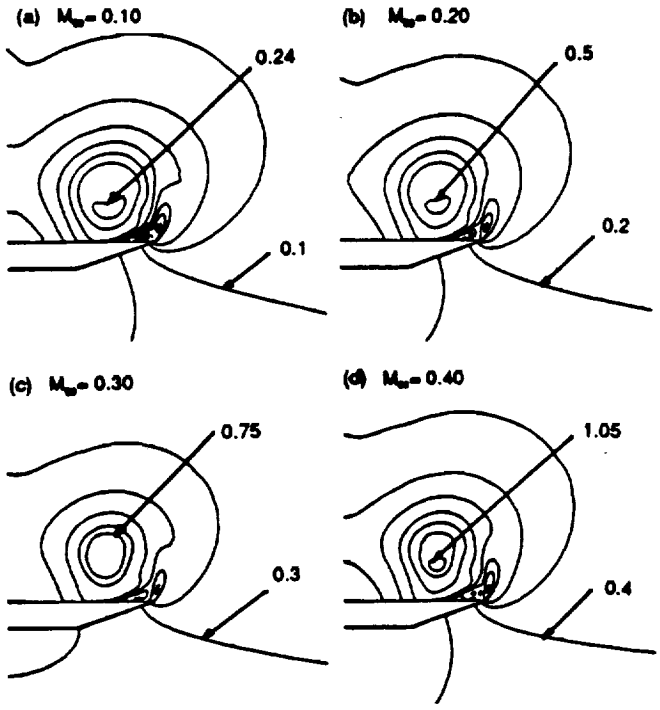

Fig 2. Effect of Freestream Mach Number on Maximum Local Mach Number, Medium Grid, $\alpha = 30°$, x/c = 0.25

The location or trajectory of the leading-edge vortex for the different Mach numbers is shown in Figure 3. Three orthogonal views of the wing are given in this figure to completely define the primary vortex location relative to the wing. Flow visualization data are also shown for comparison. The vortex location from the computed solutions was identified by locating the points of minimum total pressure in the primary vortex at each axial station. The computed vortex trajectories show an insensitivity to compressibility effects as there is good agreement with each other and with experiment in the pre-breakdown region. The figure also indicates that the vortex follows an almost linear path in the pre-breakdown regions, whereas the path becomes random beyond the breakdown. The point of minimum total pressure after breakdown is observed to enter a swirling type motion as it moves downstream. This indicates the spiral-type vortex breakdown that is usually observed on the delta wings. The experimental vortex locations are based on a visual determination of an average vortex center location, and therefore do not exhibit this swirling motion after breakdown.

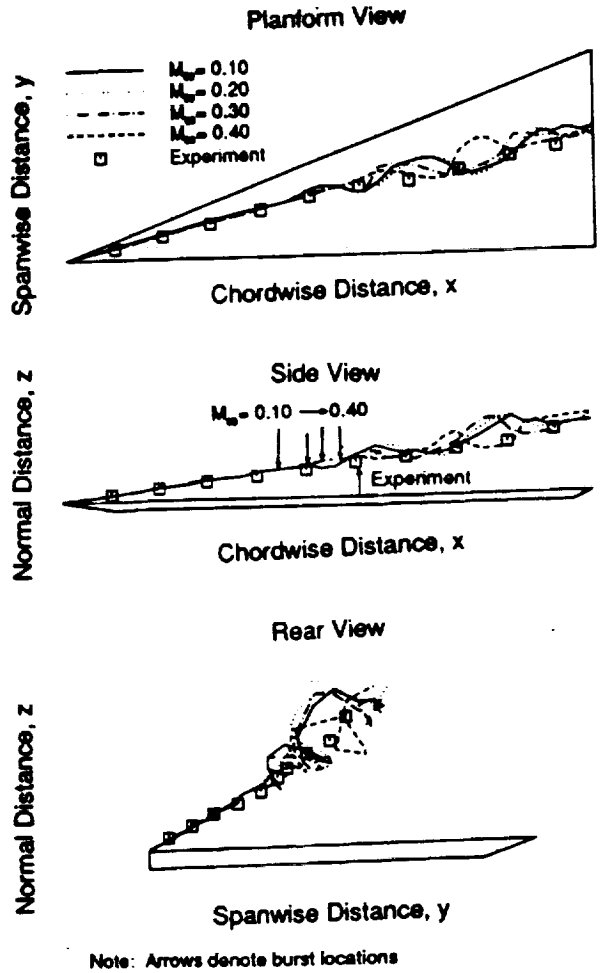

Fig. 3 Comparison of Predicted Vortex Location with Test Data, Medium Grid, $\alpha = 30°$, Re = 1 x 10^6

Figure 3 also shows that with increased freestream Mach number, the computed breakdown location moves downstream. For the cases analyzed here, the movement is as high as 10% chord. It is postulated that at higher Mach numbers there is a lesser influence of the downstream flowfield on the flowfield upstream of breakdown. Although expected to be the worst prediction of breakdown, the computed location for $M_\infty = 0.4$ yields the best agreement with the test data. This may be fortuitous, as the test data were obtained at a very low Mach number ($M_\infty \leq 0.05$). However, there are a number of other issues such as wind tunnel wall effects, transition, etc., that may have significant effects on the breakdown locations. No attempt has been made to resolve these issues in this study.

The computational breakdown locations shown in Figure 3 were obtained by examining the axial velocity contours. Ahead of breakdown, the contours usually have a symmetric structure with the maximum axial velocity residing in the well-defined core of the vortex. At axial stations further downstream, however, the core becomes more diffuse. Eventually, the contours become asymmetric with lower axial velocities at the center of the vortex than on the periphery. The breakdown location is thus determined by locating the axial station where this change in the axial velocities is first observed.

This method of determining the breakdown location has been applied successfully for delta wings, and is consistent with experimental observations (Ref 12). This method has also been used to establish a breakdown criterion for delta wings using Rossby number (Ref 13). Figure 4 shows how the Rossby number behaves along the wing chord, for the four different Mach numbers. It has been shown in Ref 13 that when the Rossby number reaches a value on the order of one, breakdown is expected to occur. Although such an observation is based on a very limited amount of experimental and computational results, the present results (Figure 4) also support such a finding. In this figure, the breakdown locations shown in Figure 3 are indicated. As can be observed, the Rossby numbers corresponding to breakdown have values near one.

Unsteady Effects

All calculations shown in this study were made using a local time stepping scheme to accelerate convergence. Thus, time-accurate solutions were not obtained. There was evidence, however, of small instabilities in the CFD solutions. These solutions were examined to determine the effects of this unsteadiness on the vortex breakdown location. It should be noted that time-accurate calculations must be performed to obtain data for a true time or frequency response analysis.

Oscillations in the integrated forces and moment histories indicate the presence of inherent flow unsteadiness at high angles of attack. Figure 5 shows typical histories of computed lift, drag, and pitching moment coefficients for $M_\infty = 0.3$. Although the solutions appear to be fairly well converged after 1000 iterations, there are oscillations in the forces and moment even after 2400 iterations. The magnitude of the oscillations are, however, on the order of 2% of their mean values. Also, further iterations on the solution did not improve the convergence. The oscillations in forces and moment are indications of inherent flow unsteadiness for such conditions. For improved predictions of vortex breakdown location, it is important to investigate the sensitivity of breakdown location to the flowfield unsteadiness.

Although time-accurate calculations should be used in obtaining the unsteady effects, they require an exorbitant amount of computation time. Therefore, a simpler ad-hoc method was sought for quantifying the effect of unsteady flow on breakdown. The Rossby number has shown promise in predicting flow unsteadiness in the vortical region. Figure 6a shows a typical history of Rossby number at a location (20% root chord) well upstream of breakdown, as the solution is executed for a freestream Mach number of 0.4. Figure 6b shows a similar history at a location (80% root chord) downstream of breakdown. Ahead of breakdown, the Rossby number approaches a nearly constant value (about 1.9) as the solution converges, implying a nearly steady flowfield. On the other hand, downstream of burst, the Rossby number does not converge. This indicates a significant amount of inherent unsteadiness in the post-breakdown region. Such an observation, steady flow upstream of burst and unsteady flow downstream of burst, is also consistent with experimental observations (Ref 17).

The effects of post-breakdown unsteadiness on vortex breakdown location may also be examined using the Rossby number. A breakdown location history determined using a critical Rossby number (assumed to be 1.0, based on Ref 13) for $M_\infty = 0.4$ is shown in Figure 7. As the solution converges, vortex breakdown first occurs at the trailing edge of the wing and then moves upstream to about 50% root chord. The breakdown location can be observed to be oscillating between chordwise grid planes over approximately 5% root chord after 2000 iterations. Although, the oscillations in burst location shown here are based on computational results using the local maximum time stepping scheme, experimental breakdown location for the 70° delta wing has also been observed to dynamically oscillate about 5% root chord for this angle of attack.

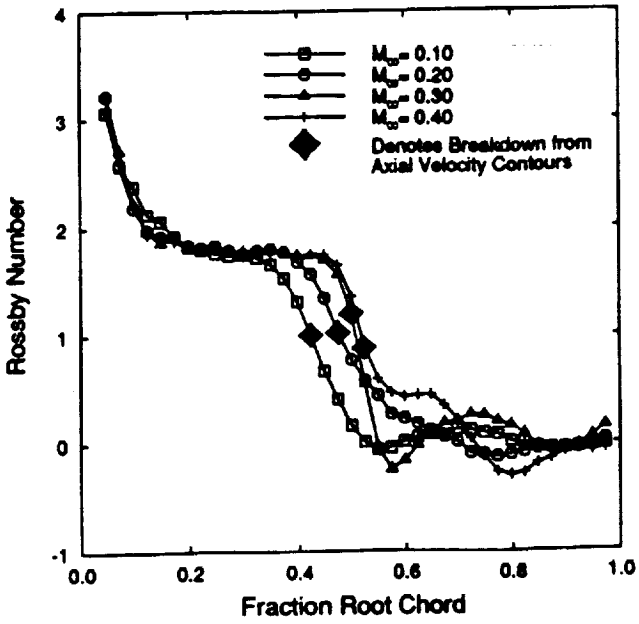

Fig. 4 Effect of Freestream Mach Number on Rossby Number Along the Chord, Medium Grid, α= 30°, Re = 1 x 10^6

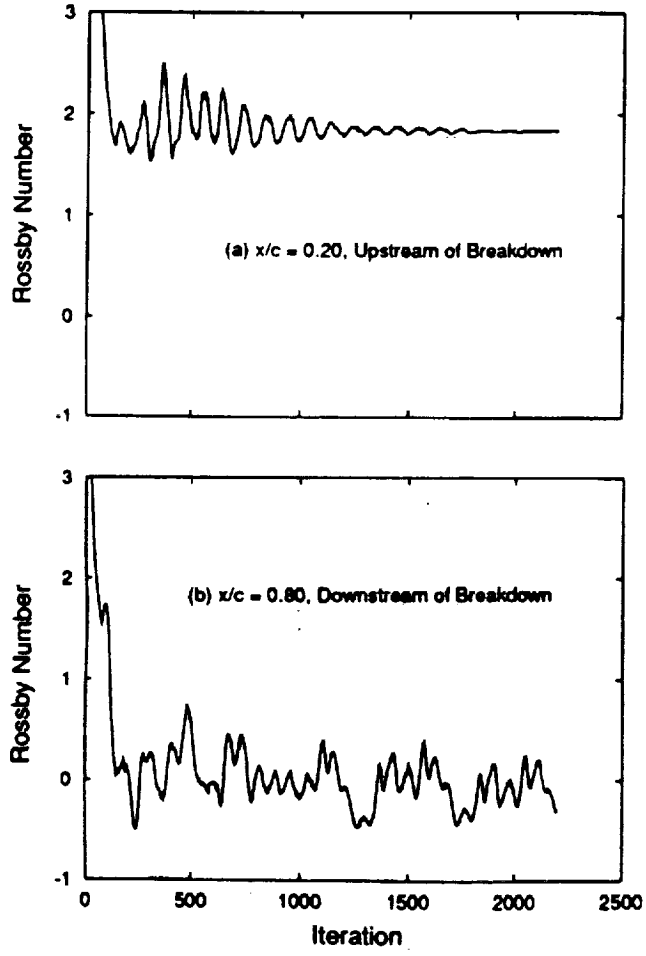

Fig 6. Typical Rossby Number Histories in Pre- and Post- Breakdown Regions, Medium Grid
M_∞= 0.4, α= 30°, Re = 1 x 10^6

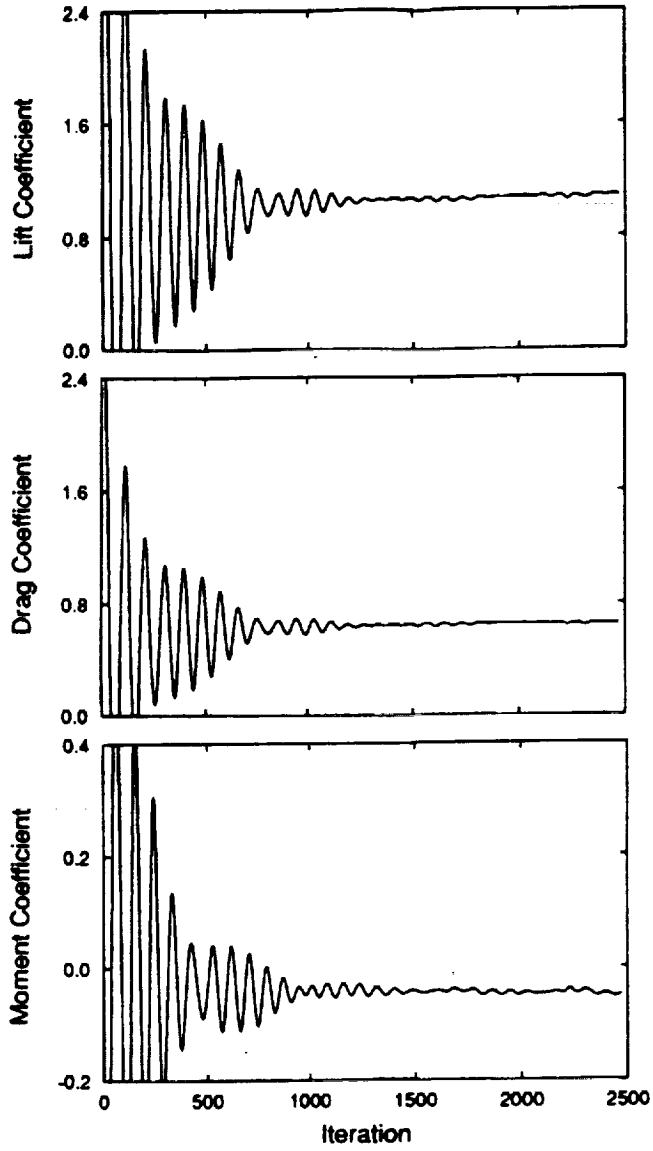

Fig. 5 Force / Moment Histories, α = 30°
M_∞= 0.30, Re = 1 x 10^6

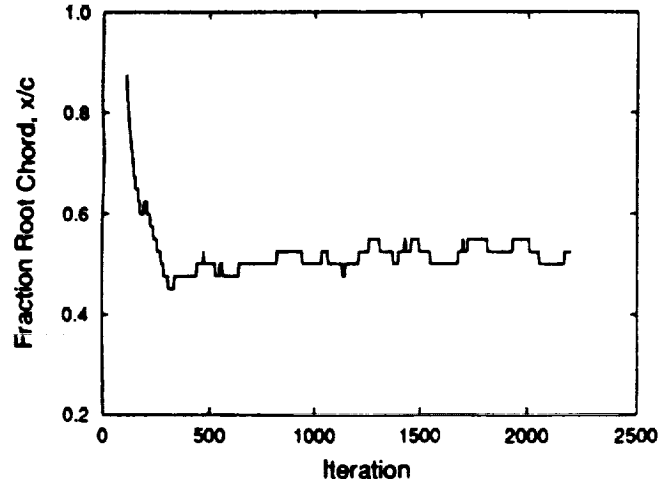

Fig. 7 Vortex Breakdown Location History Corresponding to Rossby Number = 1.0, Medium Grid
M_∞= 0.4, α= 30°, Re = 1 x 10^6

Grid Enrichment Effects

The medium grid used in this study is considered too coarse for adequate resolution of the vortical flowfields. Although only local time stepping was considered for this investigation, adequate spatial resolution of the flowfield is also necessary for time-accurate calculations. To investigate the effect of grid refinement in the vortical flow region, a grid embedding procedure was used in which a subset of the medium grid was enriched equally in all index directions. The grid was enriched over the upper surface of the wing and around the leading edge to better resolve not only the vortical flow region but also the feeding shear layer. The extent of embedding in the normal direction was just far enough to include the region where most of the vortical flow phenomena is observed. This refinement of the medium grid yielded an embedded region with dimensions 81 (axial), 87 (radial), and 133 (circumferential). Figure 8 shows the embedded region in a crossflow plane.

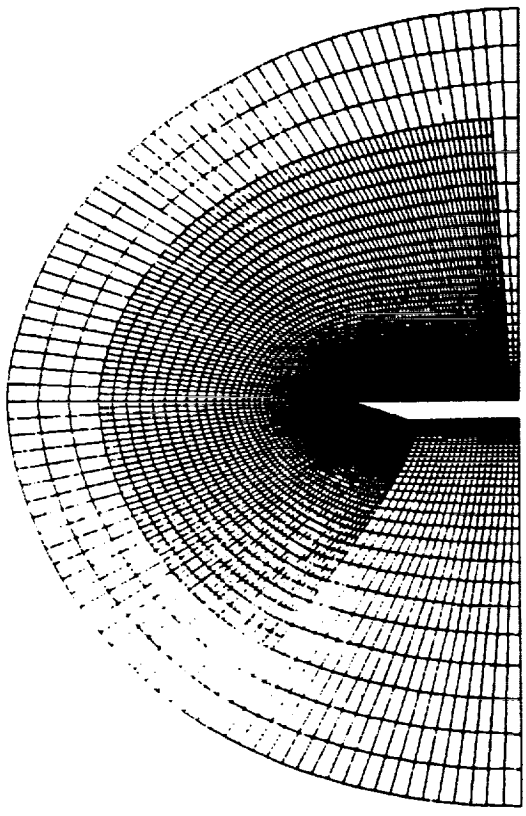

Fig. 8 Cross-Section View of the Embedded Medium Grid
Grid Dimensions in the Embedded Region: 81 x 87 x 133

The effect of grid refinement on chordwise velocity (normalized by freestream velocity) along a line parallel to the upper surface of the wing is shown in Figure 9. This line was selected to coincide with the maximum chordwise velocity in the LDV data which should be near the center of the primary vortex. Results for both medium and embedded grids are compared with the LDV data. The computed solutions underpredict the velocities compared with experiment, however, grid embedding improves the solution considerably. In general, the shape of the profile is better predicted, although the comparison with the test data is not very good. Without grid embedding, the maximum velocity at the vortex center is only about 2.3 times it's freestream value, whereas with grid embedding it is increased to about 3.0, which is closer to the experimental value of about 3.4. Also, outboard of the vortex center location, a slight flattening of the profile is due to the secondary vortex that is predicted better with grid embedding.

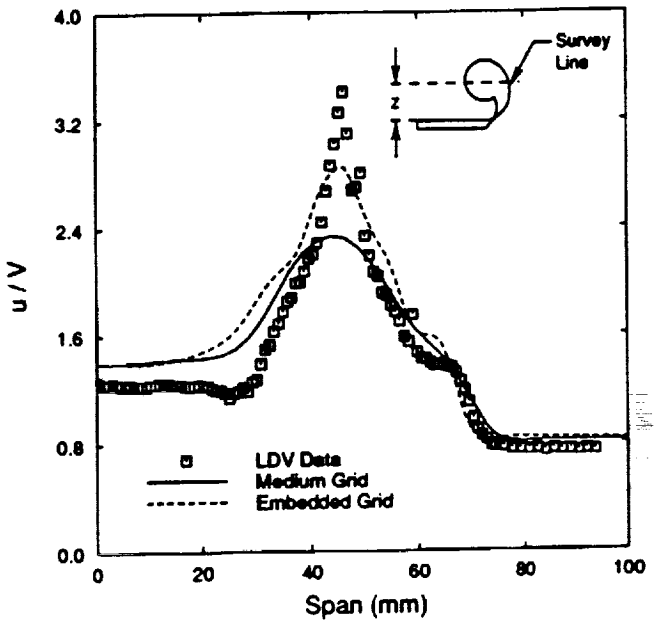

Fig. 9 Comparison of Chordwise Velocity Along a Line Parallel to the Wing Upper Surface
$M_\infty = 0.3$, $\alpha = 30^\circ$, $Re = 1 \times 10^6$, $x/c = 0.25$, $z = 25$ mm

Improved results with grid embedding can also be seen by analyzing the streamwise vorticity contours (Figure 10). These contours are shown in the pre-breakdown region (25% root chord), for both the medium and embedded grid solutions and also for the experimental data obtained using LDV. Although the computed contour levels are overall very similar to the experimental data, the maximum value of vorticity in the vortex core is nearly 5.5 times greater in the LDV data than in the computed solutions with the medium grid. Much improvement is found with the grid embedding, for which case this ratio is about 3.4. The resolution of vorticity in the secondary vortex region and in the feeding shear layer also is better with the grid embedding.

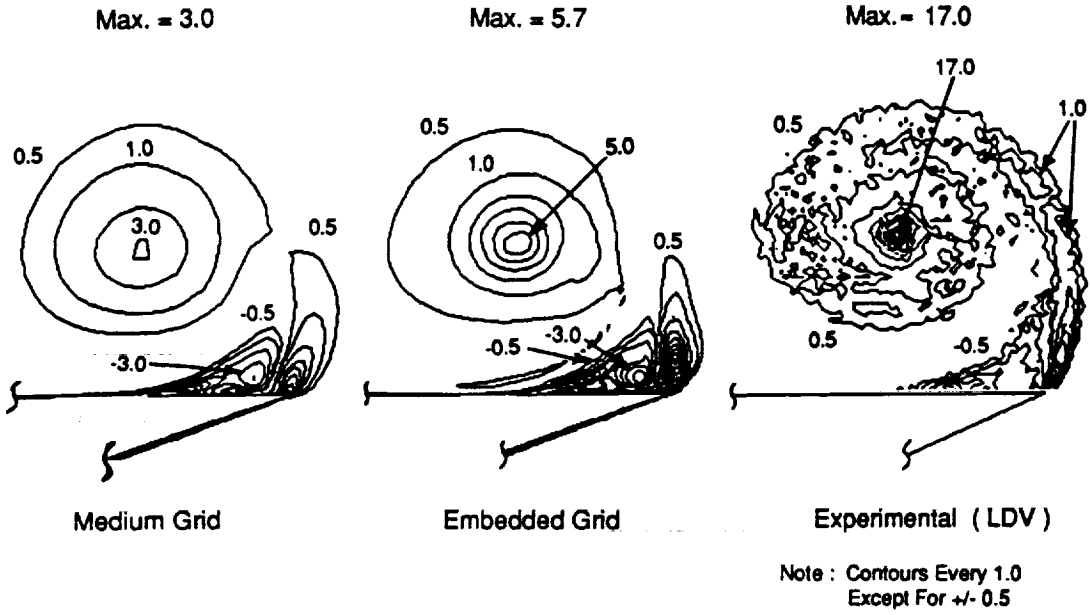

Fig. 10 Comparison of Predicted Vorticity Levels (x-Direction)
Before Burst, $M_\infty = 0.30$, $\alpha = 30°$, $Re = 1 \times 10^6$, $x/c = 0.25$

Figures 9-10 clearly demonstrate the sensitivity of the grid resolution on flowfield details in the vortical flow regions. The effect of increased grid density on breakdown location, as determined again by the Rossby number of 1.0, is shown in Figure 11. The burst location moves upstream by about 5% root chord with the grid embedding. Unlike the comparisons shown in Figures 9-10, the comparison with the experimental breakdown location has degraded with increased grid density. This discrepancy may be due to not modeling the wind tunnel walls, as the tunnel blockage was approximately 10% at 40° angle of attack.

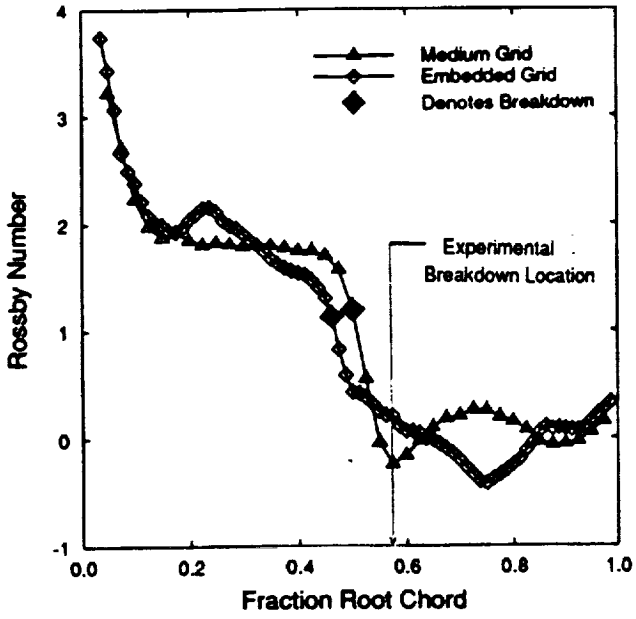

Fig. 11 Effect of Grid Embedding on Rossby Number Along the Chord, $M_\infty = 0.30$, $\alpha = 30°$, $Re = 1 \times 10^6$

Summary

Effects of Mach number, flowfield unsteadiness, and grid embedding on vortical flow structure and vortex breakdown location were analyzed using Navier-Stokes solutions on a 70° delta wing with sharp leading edge. Analysis was performed for only laminar flow based on previous investigations and in order to eliminate turbulence model effects. The computed results were compared with an experimental database obtained at low subsonic speeds. The computational solutions, in general, showed very good agreement with the test data as far as the vortex trajectories were concerned. However, mixed results were obtained for the streamwise vorticity, velocities near the vortex core, and vortex breakdown locations.

For freestream Mach numbers above 0.3, the computed flow in the core of the vortex was found to be well into the compressible range ($M_\infty \geq 0.7$). In fact, for $M_\infty = 0.4$ it reached the sonic condition. With the increase in freestream Mach number, the breakdown location moved downstream. The movement was as high as 10% of the root chord for the cases investigated. It is postulated that at higher Mach numbers there is a lesser influence of the downstream flowfield on the flowfield upstream of breakdown.

Oscillations in forces and moment after a few thousand iterations were used as indications of unsteadiness in the flowfield. Although oscillations in forces were less than 2% of their mean values, the breakdown location was found to wander over approximately 5% of the root chord. This was consistent with the test data.

Prediction of the chordwise velocity near the vortex core was improved with grid embedding. Without grid embedding, the maximum velocity at the vortex center was only about 2.3 times its

freestream value, whereas with grid embedding it was increased to about 3.0, the experimental value being 3.4. Prediction of streamwise vorticity contour levels was also much improved with the grid embedding. The maximum vorticity contour level increased from 3.0 to 5.0 with the increased grid resolution, experimental value being 17.0. The burst location, however, moved upstream by about 5% root chord, resulting in a degradation in correlation with test data.

The Rossby number value of about 1.0 at vortex breakdown was used in interpreting the majority of results in this study, and provided a useful method for fast determination of vortex breakdown locations. Other issues such as effects of wind tunnel walls, transition, and turbulence modeling still remain unresolved.

Acknowledgement

This study was supported by the McDonnell Douglas Independent Research and Development program. Computer resources for this work were provided by the National Aerodynamic Simulation facility as part of a study sponsored by Terry Holst of NASA Ames Research Center. Experimental data was obtained by MCAIR in conjunction with McDonnell Douglas Research Laboratories (MDRL) as part of a United States Navy funded investigation of leading-edge vortex behavior on delta wings.

References

1. Lambourne, N.C., and Bryer, D.W., "The Bursting of Leading-Edge Vortices - Some Observations and Discussion of the Phenomenon," A.R.C., R. & M. No. 3282, April 1961.

2. Escudier, M., "Vortex Breakdown: Observations and Explanations," Progress in Aerospace Sciences, Vol. 25, 1988, pp. 189-229.

3. Leibovich, S., "The structure of Vortex Breakdown," Annual Review of Fluid Mechanics, Vol. 10, 1978, pp. 221-246.

4. Leibovich, S., "Vortex Stability and Breakdown: Survey and Extension," AIAA Journal, Vol. 22, No. 9, September 1984, pp. 1192-1206.

5. Wentz, W.H., and Kohlman, P.L., "Wind Tunnel Investigations of Vortex Breakdown on Slender Sharp-Edged Wings," NASA Research Grant NGR-17-002-043, Final Report, November 1968.

6. McKernan, J.F., and Nelson, R.C., "An Investigation of the Breakdown of the Leading Edge Vortices on a Delta Wing at High Angles of Attack," AIAA-83-2114, August 1983.

7. Kegelman, J.T., and Roos, F.W., "Effects of Leading-Edge Shape and Vortex Burst on the Flowfield of a 70-degree-Sweep Delta Wing," AIAA-89-0086, January 1989.

8. Hitzel, S.M., "Wing Vortex Flows Up Into Vortex Breakdown, A Numerical Similation," AIAA-88-2518-CP, June 1988, pp. 73-83.

9. O'Neil, P.J., Barnett, R.M., and Louie, C.M., "Numerical Solution of Leading-Edge Vortex Breakdown Using an Euler Code," AIAA-89-2189, July 1989. (also to appear in Journal of Aircraft).

10. Hartwich, P.M., Hsu, C.H., Luckring, J.M., and Liu, C.H., "Numerical Study of the Vortex Burst Phenomenon for Delta Wings," AIAA-88-0505, January 1988.

11. Ekaterinaris, J.A., and Schiff, L.B., " Vortical Flows over Delta Wings and Numerical Prediction of Vortex Breakdown," AIAA-90-0102, January 1990.

12. Agrawal, S., Barnett, R.M., and Robinson, B.A., "Investigation of Vortex Breakdown on a Delta Wing Using the Euler and Navier-Stokes Equations," AGARD-FDP Symposium on Vortex Flow Aerodynamics, AGARD-CP-494, Paper No. 24, July 1991. (also to appear in AIAA Journal).

13. Robinson, B.A., Barnett, R.M., and Agrawal, S., "A Simple Criterion for Vortex Breakdown," AIAA-92-0057, January 1992.

14. Thomson, J.F., Thames, F.C., and Mastin, C.W., "Automatic Numerical Generation of Body-Fitted Curvilinear Coordinate System for Field Containing Any Number of Arbitrary Two-Dimensional Bodies," Journal of Computational Physics, Vol. 15, No. 3, July 1974, pp. 299-319.

15. Thomas, J.L., Taylor, S.L., and Anderson, W.K., "Navier-Stokes Computations of Vortical Flows Over Low Aspect Ratio Wings," AIAA-87-0207, January 1987.

16. Batchelor, G.K., "An Introduction to Fluid Dynamics," Cambridge University Press, 1967.

17. O'Neil, P.J., Roos, F.W., Kegelman, J.T., Barnett, R.M., and Hawk, J.D., "Investigation of Flow Characteristics of a Developed Vortex," Final Report, NADC-89114-60, May 1989.